Compressible boundary layers over wavy walls

Spyridon G. Lekoudis, Ali H. Nayfeh, and William S. Saric

Citation: Physics of Fluids (1958-1988) **19**, 514 (1976); doi: 10.1063/1.861507
View online: http://dx.doi.org/10.1063/1.861507
View Table of Contents: http://scitation.aip.org/content/aip/journal/pof1/19/4?ver=pdfcov
Published by the AIP Publishing

Compressible boundary layers over wavy walls

Spyridon G. Lekoudis, Ali H. Nayfeh, and William S. Saric

Virginia Polytechnic Institute and State University, Blacksburg, Virginia 24061
(Received 9 June 1975; final manuscript received 24 December 1975)

An analysis is presented of compressible viscous flows past wavy walls without restricting the mean flow to be linear in the disturbance layer. Linearization of the compressible disturbance equations results in a system of six first-order differential equations for the perturbation quantities. The method of orthonormalization is used to control the error growth in the numerical solution of these equations. The present results agree more closely with experimental data than the results obtained by using Lighthill's theory, which restricts the mean flow to be linear in the disturbance layer.

I. INTRODUCTION

The present study is a linear analysis of compressible boundary-layer flows over wavy walls.

This problem finds applications in different areas such as transpiration cooling of re-entry vehicles and rocket boosters, cross hatching on ablative surfaces, and film vaporization in combustion chambers. The present analysis can determine increased heat transfer due to wall roughness. It also provides the mean flow for stability analyses of flows over wavy walls.

Ackeret[1] treated compressible inviscid flows over wavy walls and pointed out the difference between the behavior of subsonic and supersonic flows. In his analysis of shock wave/boundary layer interaction, Lighthill[2] extended the work of Ackeret by including the effects of viscosity in both the mean and disturbed flows. However, he confined the effects of viscosity on the disturbance to a small sublayer near the wall. Within this sublayer the mean-flow velocity is assumed to vary linearly with the distance from the wall. Inger[3] extended the analysis of Lighthill by accounting for heat transfer effects. Whereas Lighthill and Inger determined their solutions by using *ad hoc* methods, Bordner *et al.*[4] obtained their solution by using the method of composite expansions (see, for example, Sec. 4.2 of Ref. 5). Instead of using a semianalytical technique, Fannelöp and Flügge-Lotz[6] determined a numerical solution by using finite differences and ascertained the effects of the wall waviness on the displacement thickness and the position of separation.

Benjamin[7] carried out an analysis for incompressible flows over flexible walls and pointed out that the mean flow may not be linear in the viscous sublayer for turbulent flows because of the large slopes involved.

In this paper, we use a semianalytical technique to determine compressible viscous flows past wavy walls without restricting the mean flow to be linear in the disturbance sublayer. Comparisons are made with the experiments of Inger and Williams.[8]

II. PROBLEM FORMULATION

We consider a two-dimensional steady compressible flow over a wavy wall having the equation (see Fig. 1)

$$y^* = \epsilon^* \cos k^* x^*. \tag{1}$$

For simplicity, the gas is assumed to be perfect and its viscosity μ^* is assumed to be related to the temperature T^* by the Sutherland law. Dimensionless quantities are introduced as follows:

$$\begin{aligned} &x = k^* x^*, \quad && y = k^* y^*, \quad && u = u^*/U_e^*, \\ &v = v^*/U_e^*, \quad && p = p^*/\rho_e^* U_e^{*2}, \quad && \rho = \rho^*/\rho_e^*, \\ &T = T^*/T_e^*, \quad && \mu = \mu^*/\mu_e^*, \end{aligned} \tag{2}$$

where x^* and y^* are distances along and normal to the position of the mean wall, respectively, u^* and v^* are the corresponding velocity components, p^* is the pressure, ρ^* is the density, and the subscript e denotes free-stream conditions. Starred and unstarred quantities correspond to dimensional and dimensionless quantities, respectively.

We assume that each flow quantity is the sum of two parts, a mean part corresponding to a parallel mean flow and a small-disturbance part. The parallel mean flow assumption limits the applicability of the present results to subsonic and moderately supersonic flows as shown by Lees and Reshotko[9] and Brown.[10] Equation (1) demands that any linear disturbance must vary sinusoidally with the axial distance. Hence, we can express the flow quantities as:

$$\begin{aligned} u(x, y) &= U_0(y) + \epsilon u_1(y) e^{ix} + \text{c.c.}, \\ v(x, y) &= \epsilon v_1(y) e^{ix} + \text{c.c.}, \\ T(x, y) &= T_0(y) + \epsilon T_1(y) e^{ix} + \text{c.c.}, \\ p(x, y) &= P_0 + \epsilon p_1(y) e^{ix} + \text{c.c.}, \\ \rho(x, y) &= \rho_0(y) + \epsilon \rho_1(y) e^{ix} + \text{c.c.}, \end{aligned} \tag{3}$$

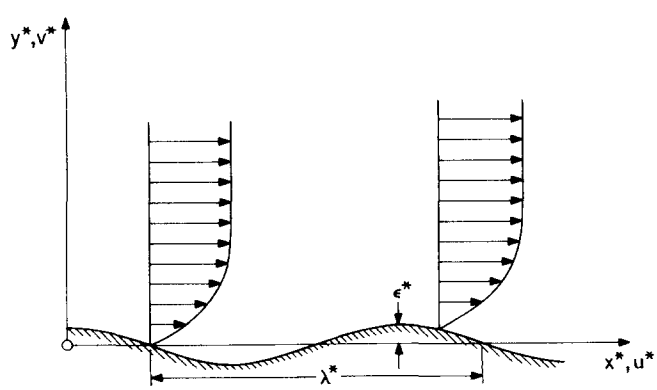

FIG. 1. Flow configuration.

where $\epsilon = \epsilon^* k^*$ and c.c. stands for the complex conjugate of the preceding terms. Substituting Eqs. (3) into the compressible Navier–Stokes equations, subtracting the mean-flow quantities, keeping only linear disturbance terms, and in the case of turbulent flows making the assumption of quasi-laminar behavior (the turbulent field and the disturbance quantities are uncorrelated) in the disturbance field,[11] we can express the disturbance equations in the form

$$\frac{dz_1}{dy} = z_2, \tag{4}$$

$$\frac{dz_2}{dy} = \left(1 + i\,\frac{R\rho_0 U_0}{\mu_0}\right) z_2 - \frac{\mu_0'}{\mu_0}\, z_2 + \left(\frac{R\rho_0 U_0'}{\mu_0} - i\frac{\mu_0'}{\mu_0} + \frac{\rho_0'}{3\rho_0}\right) z_3 + \left(\frac{iR}{\mu} - \frac{\gamma U_0 M^2}{3}\right) z_4 + \left(-\frac{\alpha U_0''}{\mu_0} + \frac{U_0}{3T_0}\right) z_5 - \frac{\alpha U_0'}{\mu_0}\, Z_6, \tag{5}$$

$$\frac{dz_3}{dy} = (-i)\, z_1 + \left(-\frac{\rho_0'}{\rho_0}\right) z_3 - i\gamma U_0 M^2 z_4 + \frac{iU_0}{T_0}\, z_5, \tag{6}$$

$$\frac{dz_4}{dy} = \frac{1}{\left(R + \frac{4i}{3}\,\mu_0 \gamma U_0 M^2\right)} \left(-2i\mu_0' + 4i\,\frac{\mu_0\rho_0'}{3\rho_0}\right) z_1 - i\mu_0 z_2 + \left[-iR\rho_0 U_0 - \mu_0 - \frac{\rho_0'}{\rho_0}\left(\tfrac{4}{3}\mu_0' - \frac{4\mu_0\rho_0'}{3\rho_0}\right)\right] z_3 + \left[i\gamma U_0 M^2 \left(\frac{4\mu_0\rho_0'}{3\rho_0} - \tfrac{4}{3}\mu_0'\right)\right] z_4 + \left[\frac{4}{3}\,\frac{iU_0}{T_0}\left(\mu_0' - \frac{\mu_0\rho_0'}{\rho_0}\right) + \alpha U_0'\right] z_5 + \frac{4i\mu_0 U_0}{3T_0}\, z_6, \tag{7}$$

$$\frac{dz_5}{dy} = z_6, \tag{8}$$

$$\frac{dz_6}{dy} = -2U_0' \Pr z_2 + \left(\frac{R\Pr\rho_0 T_0'}{\mu_0(\gamma-1)M^2} - 2i\Pr U_0'\right) z_3 - \frac{iU_0 R\Pr}{\mu_0}\, z_4 + \left(\frac{i\rho_0 U_0 R\Pr}{\mu_0(\gamma-1)M^2} + 1 - \frac{\alpha}{\mu_0}\, T_0'' - \frac{\Pr U_0'\alpha}{\mu_0}\right) z_5 - \frac{\mu_0' + \alpha T_0'}{\mu_0}\, z_6, \tag{9}$$

where

$$z_1 = u_1(y), \quad z_2 = du_1/dy, \quad z_3 = v_1(y), \quad z_4 = p_1(y), \quad z_5 = T_1(y), \quad z_6 = dT_1/dy, \tag{10}$$

and

$$R = U_e^* \rho_e^* / k^* \mu_e^*, \quad \Pr = C_p^* \mu_e^* / \kappa^*, \quad M = U_e^* / (\gamma^* R^* T^*)^{1/2}, \quad \alpha = \left(\frac{3}{2T_0} - \frac{1}{T_0 + c/T_e^*}\right)\mu_0 \tag{11}$$

Since hypersonic flows are excluded, the present analysis can be applied to the three-dimensional compressible flows past wavy walls by using a sweep back angle as demonstrated by Inger.[3]

At the wall the no-slip and no-penetration conditions yield the boundary conditions

$$u_1 = -dU_0/dy \text{ at } y = 0, \tag{12}$$

and

$$v_1 = 0 \text{ at } y = 0. \tag{13}$$

For the temperature perturbation, we assume either an isothermal wall

$$T_1 = -dT_0/dy \text{ at } y = 0, \tag{14}$$

or a constant heat-transfer rate

$$dT_1/dy = -d^2 T_0/dy^2 \text{ at } y = 0. \tag{15}$$

In arriving at these boundary conditions, the actual boundary conditions were transferred to the mean position of the wall. This is justified when $\epsilon \ll 1$; that is, when the amplitude ϵ^* of the disturbance is small compared with the disturbance wavelength λ^*. Since the flow is viscous, all disturbances must tend to zero as $y \to \infty$.

To determine the rate at which the disturbances decay as $y \to \infty$, we note that the mean-flow quantities become constants as $y \to \infty$ and Eqs. (4)–(9) reduce to the following system of equations with constant coefficients:

$$dz/dy = Az, \tag{16}$$

where z is a 6×1 matrix and A is a 6×6 matrix that is defined in Appendix A. Equations (16) admit solutions of the form

$$z_i = \sum_{j=1}^{6} c_{ij} \exp(\lambda_j y) \text{ for } i = 1, 2, \ldots, 6, \tag{17}$$

where the c_{ij} are constants and the λ_j are the eigenvalues of the system

$$|A - \lambda I| = 0. \tag{18}$$

These roots are consistent with those obtained by Lees and Reshotko[9] and Mack.[12] Since A is a 6×6 matrix, Eq. (18) has six roots. Three of these roots have positive real parts and the other three have negative real parts as shown in Appendix B. In order that the disturbance vanish away from the wall, the solutions that grow exponentially with y must be discarded. This leaves three linear independent solutions that decay exponentially with y. Hence, as $y \to \infty$, the boundary conditions are taken in the form

$$Dz = 0 \text{ at } y = y_0, \tag{19}$$

where y_0 is any value larger than the boundary-layer thickness and D is a 6×3 constant coefficient matrix that is defined in Appendix C.

III. COMPUTATIONAL PROCEDURE

The first step in the computational procedure is the generation of the elements of the matrix A of Eq. (16). These coefficients depend on the mean flow.

For laminar flows, the mean-flow profiles are generated by using the Illingworth–Stewartson transformation,[13] which leads to a second-order integrodifferential equation. This equation is then solved by using finite differences. It is worthwhile to note the excellent stability of the Thomas algorithm and the insensitivity of the solution of this equation to the step size of integration. A representative of these calculations is shown in Fig. 2.

For turbulent flows, the mean-flow profiles are cal-

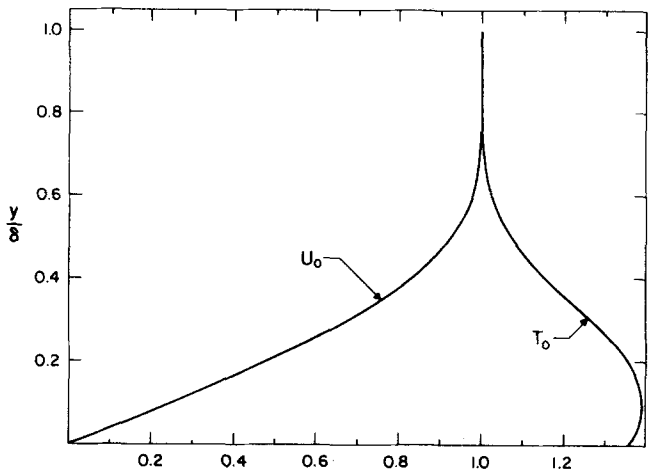

FIG. 2. A representative laminar boundary-layer profile ($M = 2.0$, $\delta^* = 2$ cm, $T_w^*/T_{ad}^* = 0.8$).

culated by using the method of Inger[3] who used a similarity solution with an approximate Crocco integral for temperature. A representative of these calculations is shown in Fig. 3.

Once the mean profile is calculated, A, dU_0/dy, dT_0/dy, and d^2T_0/dy^2 can be determined. Thus, the problem is reduced to the solution of the system of six first-order differential equations (4)–(9) subject to the boundary conditions (12), (13), (19), and either (14) or (15).

A straightforward integration of Eqs. (4)–(9) utilizing superposition of solutions fails because of parasitic errors among the six solutions. Since the real parts of the eigenvalues of A are well separated, one cannot continue to accurately calculate six linearly independent solution vectors of Eqs (4)–(9). This can easily be seen from Eq. (17). If two of the λ_j differ by a factor of 10, one solution grows by the factor $\exp(10n\Delta y)$ relative to the other, as one integrates n steps toward the wall. Thus, a 10^{-12} roundoff error may quickly dominate the solution. These characteristics are similar to those encountered in the solution of the Orr–Sommerfeld equation, and thus one can use one of the techniques that has been successfully used for its solution. One method which can eliminate this difficulty is the orthonormalization of the solutions of the set of equations whenever a loss of independence is detected. In this paper, we use a technique developed by Scott and Watts.[14]

To reduce the computational time while keeping reasonable accuracy, we use a fifth-order Runge–Kutta routine to perform two integrations, the step size used in one of them is twice the step size used in the other. Comparing the results of these integrations, we determine a "global error" based on the difference between the results of these integrations. If this error is less than a prescribed value, the integration is continued and orthonormalization is not needed. However, if the global error is above the prescribed value, the solution vectors are orthonormalized and then the integration is continued. The orthonormalization is carried out using a modified Gram–Schmidt method.

The number of orthonormalizations needed depends on the eigenvalues of A, the Reynolds number being the main factor. For laminar mean-flows, about eight orthonormalizations are needed requiring about 5 min on an IBM 370/158 computer. For turbulent mean flows, we examined cases where up to 150 orthonormalizations were needed requiring about 40 min. Application of the free-stream boundary conditions at different y stations was used as a check.

IV. RESULTS AND DISCUSSION

Lighthill[2] examined the interaction of shock waves with a boundary layer. Inger,[3] analyzing compressible flow over wavy walls, extended the analysis of Lighthill by including the effects of heat transfer. Their analyses are based on the assumption that the mean-flow profiles are linear within the disturbance sublayer. Figures 2 and 3 show that this assumption is invalid unless the disturbance sublayer is extremely thin in comparison with the mean boundary layer, especially for turbulent mean flows. Figure 4 shows that, for

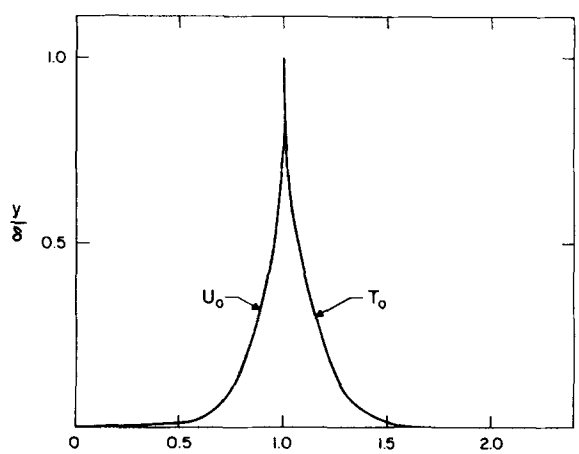

FIG. 3. A representative turbulent boundary-layer profile ($M = 2.0$, $\delta^* = 1.27$ cm, $T_w^* \approx T_{ad}^*$).

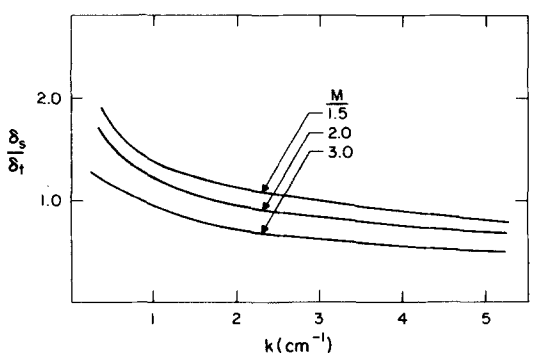

FIG. 4. Variation of the ratio of the thicknesses of the disturbance and mean sublayers, with the wavenumber ($\delta = 1.27$ cm, $T_w \approx T_{ad}$).

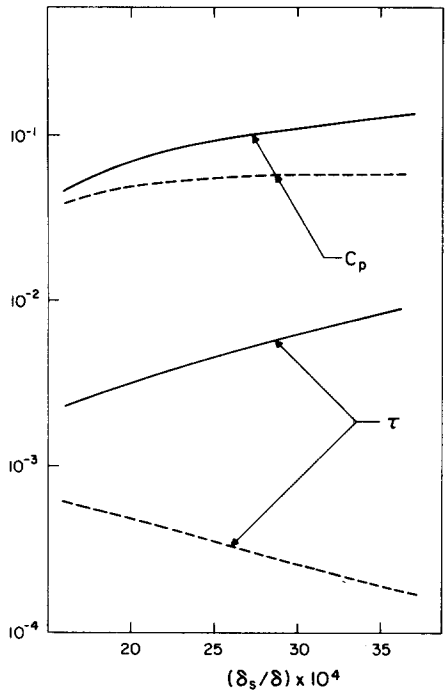

FIG. 5. Variation of the amplitude of the pressure and the shear perturbations with the sublayer thickness ($\delta = 1.27$ cm, $T_w \approx T_{ad}$, $M = 1.5$, ----Lighthill, ——present).

large wavelengths, the laminar sublayer in a turbulent boundary layer can be thinner than the disturbance sublayer.

In Figs. 5 and 6, we investigate the validity of the assumption that the turbulent mean-flow profiles are linear within the disturbance sublayer. To this end, we

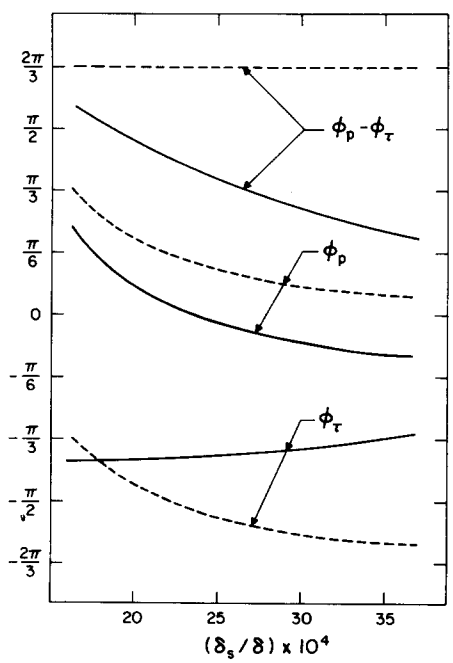

FIG. 6. Variation of the positions of the maximum pressure and shear perturbations with the sublayer thickness ($\delta = 1.27$ cm, $T_w \approx T_{ad}$, $M = 1.5$, ----Lighthill, ——present).

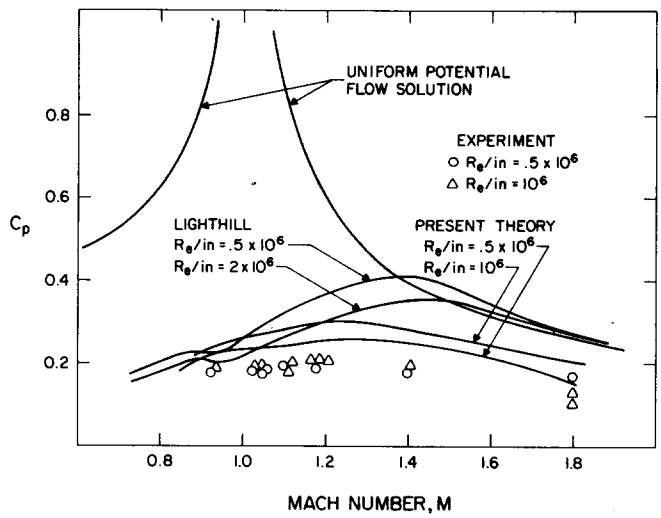

FIG. 7. Variation of the pressure coefficient with the Mach number.

show the variations of the amplitudes of the pressure and shear perturbations with the ratio of the thicknesses of the disturbance sublayer and the mean boundary layer as calculated from both the Lighthill and the present analysis. It is clear from Fig. 5 that Lighthill's theory is valid only for very small values of δ_s/δ. When $(\delta_s/\delta) \approx 35 \times 10^{-4}$, there is an order-of-magnitude difference between the amplitudes of the shear perturbations calculated from the Lighthill and the present analysis. As δ_s/δ increases, the magnitude of the difference increases rapidly. Figure 6 shows the variations of the positions of the maximum pressure and shear perturbations with δ_s/δ. This figure shows that there are also large differences between the values calculated from Lighthill's theory and our results for values of δ_s/δ as small as 20×10^{-4}. Whereas Lighthill's theory predicts that $\Phi_p - \Phi_s = 120°$, regardless of the value of δ_s/δ, our results show that $\Phi_p - \Phi_s$ is a strong function of δ_s/δ as shown in Fig. 6. Thus, the assumption that the

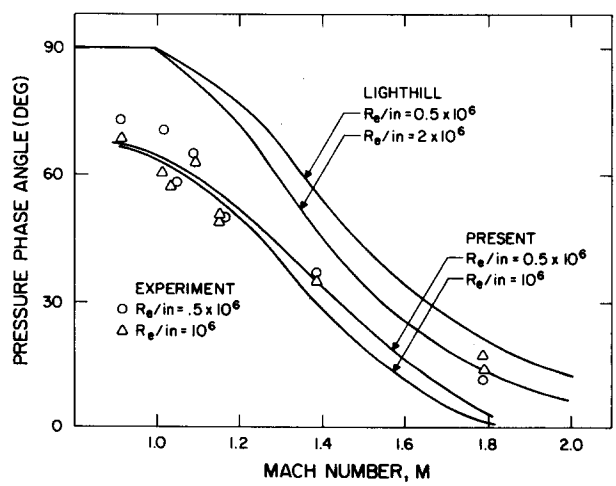

FIG. 8. Variation of the position of the maximum pressure with Mach number.

mean-flow profiles are linear in the disturbance sublayer is valid only for very small values of δ_s/δ.

Inger and Williams[8] presented experimental data for the pressure perturbations exerted by a compressible flow on a wavy wall. Figures 7 and 8 compare the experimental amplitudes and phases of the pressure perturbations with those calculated from both Lighthill's theory and our theory. These figures show clearly that our analysis is an improvement over Lighthill's theory, especially for the phase angle. We note that as the Mach number increases, the maximum pressure predicted by the present theory approaches its supersonic position faster than the maximum pressure predicted by Lighthill's theory.

Figures 9 and 10 show that in the case of laminar flows, the assumption of linear profiles within the disturbance sublayer is valid for quite large values of δ_s/δ compared with the case of turbulent flows, as expected.

ACKNOWLEDGMENTS

The comments and suggestions of Dr. D. T. Mook are greatly appreciated.

This work was supported by the Fluid Dynamics Program of the Office of Naval Research.

APPENDIX A

$$a_{11}=a_{13}=a_{14}=a_{15}=a_{16}=0,\quad a_{12}=1 \tag{A1}$$

$$a_{21}=1+iR,\quad a_{22}=a_{23}=0,\quad a_{24}=-\tfrac{1}{3}\gamma M^2+iR,$$
$$a_{25}=\tfrac{1}{3},\quad a_{26}=0 \tag{A2}$$

$$a_{31}=-i,\quad a_{32}=a_{33}=0,\quad a_{34}=-i\gamma M^2, a_{35}=i,\quad a_{36}=0 \tag{A3}$$

$$a_{41}=0,\quad a_{42}=-i/(R+\tfrac{4}{3}i\gamma M^2),\ a_{43}=(-1-iR)/(R+\tfrac{4}{3}i\gamma M^2),$$
$$a_{44}=a_{45}=0,\quad a_{46}=\tfrac{4}{3}i \tag{A4}$$

$$a_{51}=a_{52}=a_{53}=a_{54}=a_{55}=0,\quad a_{56}=1 \tag{A5}$$

$$a_{61}=a_{62}=a_{63}=0,\quad a_{64}=-iR\mathrm{Pr},\quad a_{65}=iR\mathrm{Pr}/(\gamma-1)M^2,$$
$$a_{66}=0. \tag{A6}$$

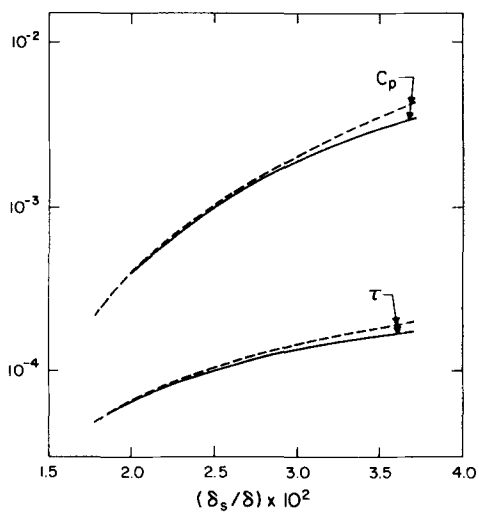

FIG. 9. Variation of the amplitude of the pressure and the shear perturbations with the sublayer thickness ($\delta=2$ cm, $T_w/T_{ad}=0.8$, $M=5.0$, ---- Lighthill, —— present).

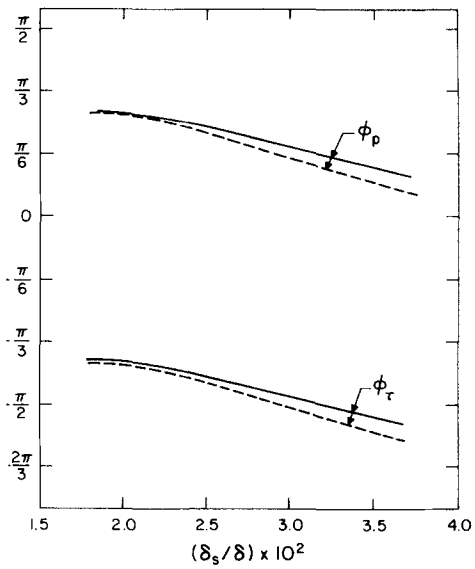

FIG. 10. Variation of the positions of the maximum pressure and shear perturbations with the sublayer thickness ($\delta=2$ cm, $T_w/T_{ad}=0.8$, $M=5.0$, ---- Lighthill, —— present).

APPENDIX B

$$\lambda_{1,2}=\pm\{1+iR\}^{1/2} \tag{B1}$$

$$\lambda_{3,5}=\pm\{\tfrac{1}{2}(\chi_{22}+\chi_{33})+[\tfrac{1}{4}(\chi_{22}-\chi_{33})^2+\chi_{32}\chi_{23}]^{1/2}\}^{1/2} \tag{B2}$$

$$\lambda_{4,6}=\pm\{\tfrac{1}{2}(\chi_{22}+\chi_{33})-[\tfrac{1}{4}(\chi_{22}-\chi_{33})^2+\chi_{23}\chi_{32}]^{1/2}\}^{1/2} \tag{B3}$$

where

$$\chi_{22}=\left(R+\frac{4i\gamma M^2}{3}\right)^{-1}(R+\tfrac{4}{3}i\gamma M^2-\gamma M^2R+\tfrac{4}{3}R\mathrm{Pr}) \tag{B4}$$

$$\chi_{33}=\left(R+\frac{4i\gamma M^2}{3}\right)^{-1}\left(R-\frac{4R\mathrm{Pr}}{3(\gamma-1)M^2}\right) \tag{B5}$$

$$\chi_{32}=-iR\mathrm{Pr} \tag{B6}$$

$$\chi_{33}=iR\mathrm{Pr}/(\gamma-1)M^2 \tag{B7}$$

APPENDIX C

The boundary conditions as $y\to\infty$ are

$$Dz=0 \tag{C1}$$

where D is a 6×3 matrix consisting of the first three rows of the matrix B^{-1}. The matrix B has the elements:

$$b_{11}=1,\quad b_{12}=\lambda_1,\quad b_{13}=-\frac{\lambda_1}{i-R},$$
$$b_{14}=b_{15}=b_{16}=0, \tag{C2}$$

$$b_{21}=B_{13},\quad b_{22}=\lambda_3B_{13},\quad b_{23}=\frac{i}{\lambda_3}(-B_{13}-\gamma M^2B_{23}+B_{33}), \tag{C3}$$

$$b_{24}=B_{23},\quad b_{25}=B_{33},\quad b_{26}=\lambda_3B_{33}, \tag{C4}$$

$$b_{31}=B_{15},\quad b_{32}=\lambda_5B_{15},\quad b_{33}=\frac{i}{\lambda_5}(-B_{15}-\gamma M^2B_{25}+B_{35}), \tag{C5}$$

$$b_{34}=B_{25},\quad b_{35}=B_{35},\quad b_{36}=\lambda_5B_{35}, \tag{C6}$$

$$b_{41}=1,\quad b_{42}=\lambda_2,\quad b_{43}=-\frac{\lambda_2}{i-R},\quad b_{44}=b_{45}=b_{46}=0, \tag{C7}$$

$$b_{51} = B_{15}, \quad b_{52} = \lambda_5 B_{15}, \quad b_{53} = \frac{i}{\lambda_5}(-B_{15} - \gamma M^2 B_{25} + B_{35}), \tag{C8}$$

$$b_{54} = B_{25}, \quad b_{55} = B_{35}, \quad b_{56} = \lambda_5 B_{35} \tag{C9}$$

$$b_{61} = B_{16}, \quad b_{62} = \lambda_6 B_{16}, \quad b_{63} = \frac{i}{\lambda_6}(-B_{16} - \gamma M^2 B_{26} + B_{36}), \tag{C10}$$

$$b_{64} = B_{26}, \quad b_{65} = B_{36}, \quad b_{66} = \lambda_6 B_{36}, \tag{C11}$$

where

$$B_{1i} = \frac{\chi_{12}(\chi_{33} - \lambda_i^2) - \chi_{13}\chi_{32}}{\chi_i^2 - \chi_{11}}, \tag{C12}$$

$$B_{2i} = \chi_{33} - \lambda_i^2, \tag{C13}$$

$$B_{3i} = -\chi_{32}. \tag{C14}$$

[1]H. W. Liepmann and A. Roshko, *Elements of Gasdynamics* (Wiley, New York, 1957), p. 208.
[2]M. J. Lighthill, Proc. R. Soc. London Ser. A 217, 478 (1953).
[3]G. R. Inger, Astronaut. Acta 16, 325 (1971).
[4]G. L. Bordner, A. H. Nayfeh, and W. S. Saric, Z. Angew. Math. Mech. (to be published).
[5]A. H. Nayfeh, *Perturbation Methods* (Wiley-Interscience, New York, 1973), Sec. 4.2.
[6]T. Fannelöp and I. Flügge-Lotz, Ing.-Arch. 33, 94 (1963).
[7]B. Benjamin, J. Fluid Mech. 6, 161 (1959).
[8]G. R. Inger and E. P. Williams, AIAA J. 10, 636 (1972).
[9]L. Lees and E. Reshotko, J. Fluid Mech. 12, 555 (1962).
[10]W. B. Brown, AIAA J. 5, 1753 (1967).
[11]W. J. Miles, J. Fluid Mech. 3, 185 (1957).
[12]L. M. Mack, in *Methods in Computational Physics*, edited by B. Alder and S. Fernbach (Academic, New York, 1965), Vol. 4, p. 247.
[13]K. Stewartson, *The Theory of Laminar Boundary Layers in Compressible Fluids* (Oxford University, Oxford, 1964), p. 61.
[14]M. R. Scott and H. A. Watts, SIAM J. Num. Anal. (to be published).